Multidimensional partial wave analysis
of SIDIS dihadron beam spin asymmetries at CLAS12

Christopher Dilks[1*] for the CLAS collaboration

Duke University, Durham, NC 27710, USA

* christopher.dilks@duke.edu

Abstract

Dihadron beam spin asymmetries provide a wide range of insights into nucleon structure and hadronization. Recent measurements at CLAS12 provide the first empirical evidence of nonzero $G_1^\perp$, the parton helicity-dependent dihadron fragmentation function (DiFF) encoding spin-momentum correlations in hadronization. These measurements also allow for a point-by-point extraction of the subleading-twist PDF $e(x)$ in a collinear framework. We observe different behavior of the asymmetries in different invariant mass regions, motivating a fully multidimensional study. The DiFFs also expand in terms of partial waves, each corresponding to the interference of dihadrons of particular polarizations. Altogether a fully multidimensional partial wave analysis is needed, and this presentation will summarize the efforts and results obtained thus far.

1 Introduction

Semi-Inclusive Deep Inelastic Scattering (SIDIS) has proven to be a versatile technique to study the nature of the nucleon. Numerous spin-momentum and spin-spin correlations in hadronization are accessible in dihadron production from polarized SIDIS, which involves the scattering of an electron off a nucleon and the detection of the scattered electron along with a hadron pair, a dihadron [1–3]. This study focuses on semi-inclusive charged pion pairs from the $e^- p \rightarrow e^- \pi^+ \pi^- X$ process using the upgraded CEBAF Large Acceptance Spectrometer (CLAS12), extending the previous measurement [4] with a partial wave analysis, which explores correlations with dihadron angular momentum.

The SIDIS dihadron-production cross section factorizes into a Parton Distribution Function (PDF), the hard scattering of the electron and quark, and a Dihadron Fragmentation Function (DiFF), which models the formation of two hadrons from the scattered quark. Since the hard scattering cross section is calculable via perturbative QCD and QED, measurements of the

SIDIS dihadron cross section constrain the involved PDFs and DiFFs [5–8]. The presented measurement is of the beam spin asymmetry

$$A_{LU} = \frac{1}{P_B} \frac{N^+ - N^-}{N^+ + N^-}, \tag{1}$$

where $N^{\pm}$ is the dihadron yield from scattering a $\pm$ helicity electron, with helicity defined in the proton rest frame, and P_B is the electron beam polarization. Since the spin of the electron is correlated with the spin of the quark, A_{LU} is directly sensitive to spin effects in hadronization, modelled by spin-dependent DiFFs.

There are three types of DiFFs at leading twist, analogous to the three collinear PDFs: the unpolarized D_1, the quark longitudinal spin-dependent $G_1^{\perp}$, and the transverse spin-dependent $H_1^{\perp}$ and $H_1^{\sphericalangle}$. A_{LU} contains several modulations of the dihadron angles ϕ_h, ϕ_R, and θ, and the corresponding amplitudes are sensitive to different combinations of PDFs and DiFFs [1, 2]. Although transverse momentum-dependent factorization of the cross section at subleading twist is not yet proven [9], Q^2 at CLAS12 reaches down to 1 GeV^2, where twist-3 effects are non-negligible. Collinear twist-3 PDFs are significant [10], however subleading-twist DiFFs are likely subdominant [11–13].

Dependence on the angular momentum of the dihadron can be included in DiFFs via a partial wave expansion. Each term describes the interference of dihadrons of particular polarizations, for example an sp-wave involves the interference of an unpolarized s-state dihadron with a longitudinally or transversely polarized p-state dihadron. The partial waves are denoted by angular momentum eigenstates $|\ell, m\rangle$, where $\ell = 0, 1, 2$ respectively corresponds to the ss, sp, pp partial waves, and m further enumerates the polarization possibilities [3]. Higher values of ℓ are likely suppressed for the relevant mass range. Each modulation amplitude of A_{LU} corresponds to a particular partial wave term of the DiFFs, denoted by $G_1^{\perp|\ell,m\rangle}$ and $H_1^{|\ell,m\rangle}$. The presented A_{LU} measurement is focused on providing access to these partial waves, which allow insight into correlations in hadronization between the fragmenting quark spin and the dihadron angular momentum.

At twist-2, A_{LU} is sensitive to the well-constrained unpolarized PDF f_1 convolved with $G_1^{\perp|\ell,m\rangle}$ [14]. With $G_1^{\perp|\ell,m\rangle}$ chiral-even, $G_1^{\perp|\ell,-m\rangle} = G_1^{\perp|\ell,m\rangle}$ and $G_1^{\perp|\ell,0\rangle} = 0$, therefore only the three amplitudes $|1,1\rangle$, $|2,1\rangle$, and $|2,2\rangle$ are studied. The twist-3 terms of A_{LU} involve the collinear twist-3 PDF $e(x)$ coupled with $H_1^{|\ell,m\rangle}$ [2]. The recent A_{LU} measurement [4] allows for a point-by-point extraction of $e(x)$ [10], given constraints on $H_1^{\sphericalangle}$ [15, 16]. With $e(x)$ in hand, the presented measurement can constrain the partial wave terms of $H_1^{|\ell,m\rangle}$. Since $H_1^{|\ell,m\rangle}$ is chiral-odd, all nine amplitudes up to $\ell = 2$ are measured.

2 Experiment and Analysis

The measurement was performed at CLAS12, the upgrade of CLAS, at Jefferson Lab [17]. A longitudinally polarized electron beam was scattered off protons within a liquid hydrogen target. Data from a 10.6 GeV electron beam from Fall 2018, which were used in [4] with an approximate integrated charge of 35.7 mC, were combined with data from a 10.2 GeV beam from Spring 2019 (46.8 mC), with the toroid polarity such that electrons bend inward.

The event selection criteria are the same as the previous measurement [4]. Only events with $Q^2 > 1$ GeV^2, $W > 2$ GeV, and $y < 0.8$ were analyzed. The pions were required to have positive Feynman-x ($x_F > 0$) and a minimum momentum of 1.25 GeV, and the dihadron a maximum z of 0.95. Exclusive reactions were suppressed with a missing mass cut of $M_X > 1.5$ GeV. The electrons and dihadrons were detected in the forward detector region with polar scatter-
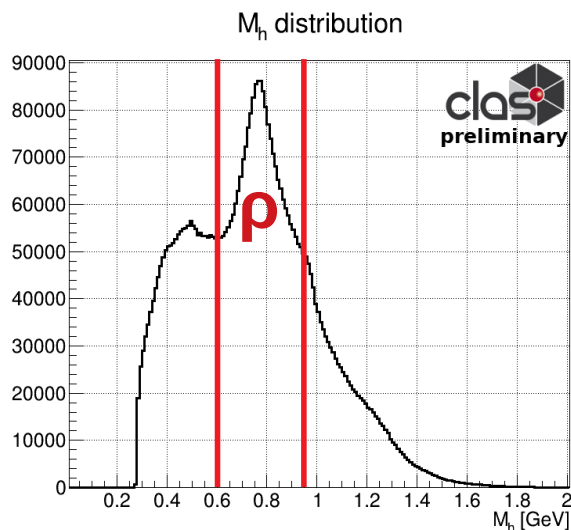
Figure 1: Invariant mass M_h distribution of $\pi^+\pi^-$ dihadrons, with the ρ^0 peak labelled. Vertical lines denote bin boundaries at 0.6 GeV and 0.95 GeV.

ing angle between 5° and 35° along with additional fiducial volume cuts, vertex cuts, and particle identification refinements.

Acceptance limitations cause the amplitudes to be linearly dependent, therefore all twelve amplitudes must be fitted for simultaneously. The twist-3 amplitudes with $m = 0$ have large fit uncertainty, since $|0,0\rangle$ and $|2,0\rangle$ are highly correlated and $|1,0\rangle$ is suppressed by the phase space; although they are excluded from the figures below, they are still included in the fit. The simultaneous fit is performed with an unbinned maximum likelihood method. The large number of parameters motivates Markov Chain Monte Carlo (MCMC) optimization for the fit, with the likelihood sequentially sampled by the Metropolis-Hastings algorithm [18–21] with a Gaussian proposal function.

3 Results

Figure 1 shows a distribution of the invariant mass M_h of the dihadrons. A prominent peak at 0.77 GeV from $\rho^0 \rightarrow \pi^+\pi^-$ decays is visible, the presence of which motivates separation of the A_{LU} measurement into three M_h bins, indicated by the vertical lines: below, around, and above the ρ^0 mass.

The A_{LU} measurements in bins of dihadron invariant mass M_h and z are shown in figures 2-5; for the full set of results including other binning schemes, refer to the presentation slides. The rows of subplots of each figure are for values of ℓ, and the columns for values of m. The label in the top-left corner of each subplot gives the partial wave eigenvalues, and the label in the top-right gives the DiFF to which the amplitude is sensitive, including subscripts for the dihadron polarizations [3]: O is for unpolarized, and L and T are for longitudinal and transverse polarization.

The leading-twist amplitudes in 12 bins of M_h are shown in figure 2. Similar to [4], a sign change is observed near the ρ^0 mass. An enhancement at the ρ^0 mass is also seen in the $|2,2\rangle$ amplitude, which corresponds to the interference of transversely polarized dihadrons. This enhancement is expected and typical of some $\ell = 2$ amplitudes. Since DiFFs are dependent on z in addition to M_h, figure 3 provides the z dependence, in the three regions of M_h described in figure 1. Different behavior is clear for the regions $M_h < 0.6$ GeV and $M_h > 0.6$ GeV, and

the amplitude magnitude tends to rise slightly as a function of z and p_T.
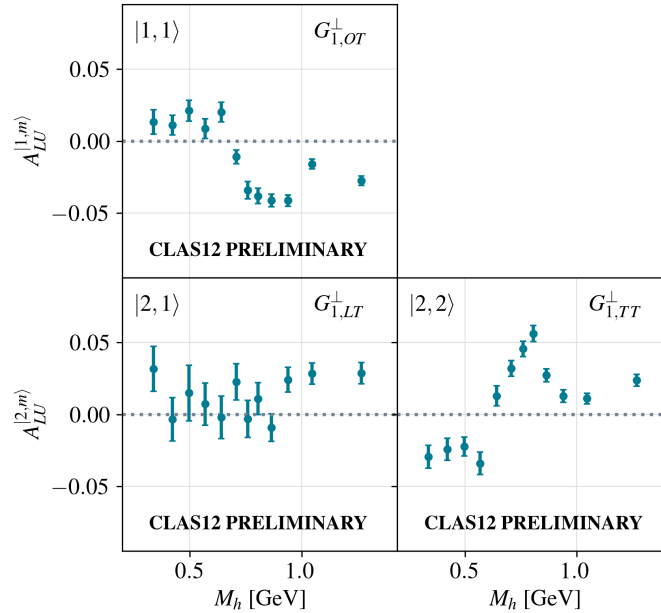
Twist-2 A_{LU} Amplitudes

Figure 2: Leading-twist A_{LU} amplitudes, in bins of M_h, sensitive to $G_1^{\perp|\ell,m\rangle}$.
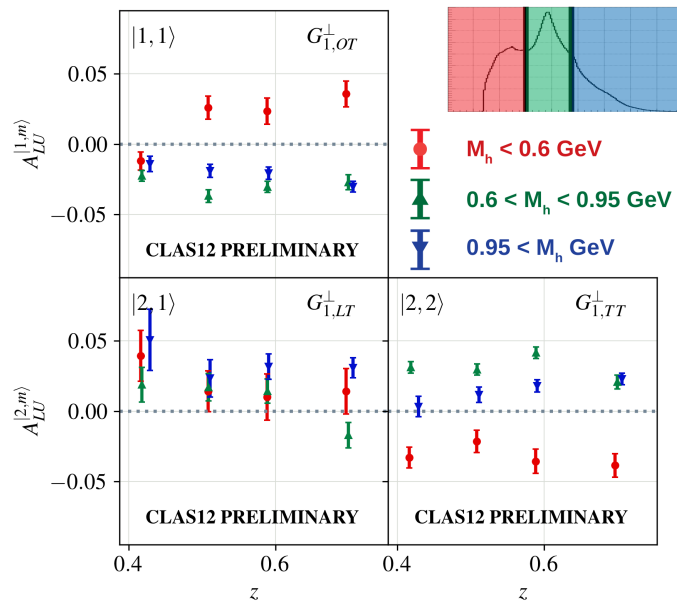
Twist-2 A_{LU} Amplitudes

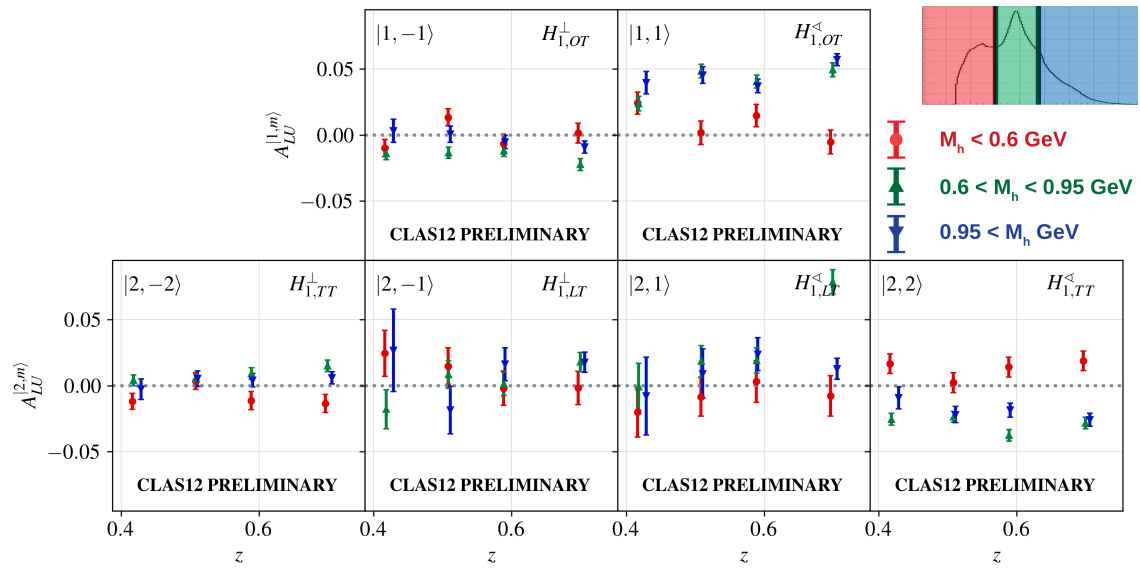Figure 3: Leading-twist A_{LU} amplitudes, in bins of z, for three regions of M_h: red circles for $M_h < 0.6$ GeV, green upward triangles for $0.6 < M_h < 0.95$ GeV, and blue downward triangles for $M_h > 0.95$ GeV. These are sensitive to $G_1^{\perp|\ell,m\rangle}$.

The twist-3 amplitudes are shown in bins of M_h in figure 4. The $|1,1\rangle$ amplitude, corresponding to sp interference, rises as a function of M_h, while the $|2,1\rangle$ and $|2,2\rangle$ amplitudes, corresponding to pp interference, show ρ^0 enhancements. Figure 5 shows the z dependence,

Twist-3 A_{LU} Amplitudes
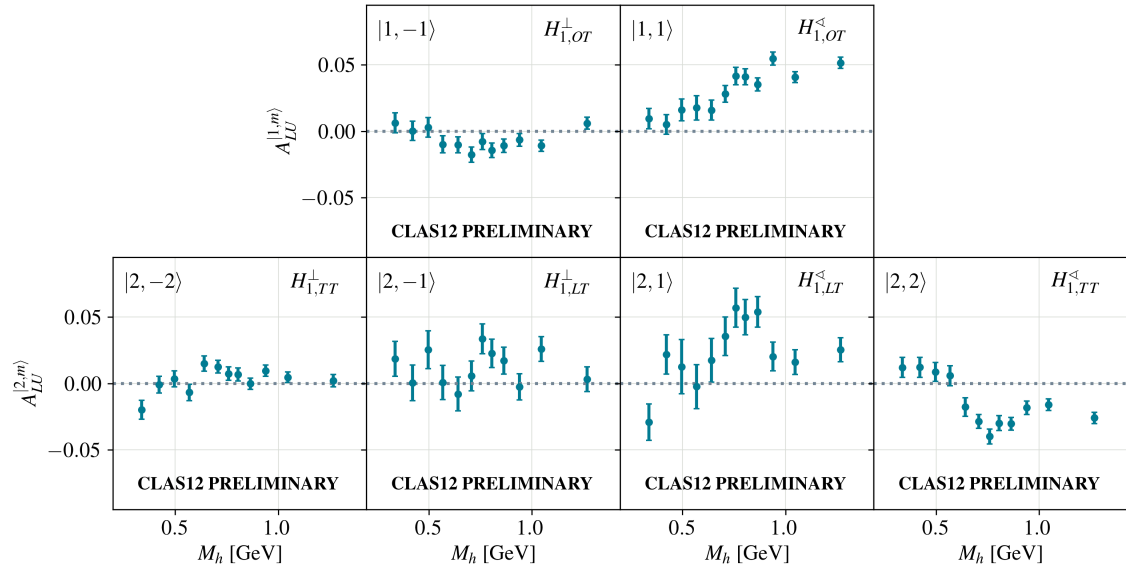
Figure 4: Twist-3 A_{LU} amplitudes, in bins of M_h, sensitive to $H_1^{|\ell,m\rangle}$.

Twist-3 A_{LU} Amplitudes

Figure 5: Twist-3 A_{LU} amplitudes, in bins of z, for three regions of M_h: red circles for $M_h < 0.6$ GeV, green upward triangles for $0.6 < M_h < 0.95$ GeV, and blue downward triangles for $M_h > 0.95$ GeV. These are sensitive to $H_1^{|\ell,m\rangle}$.

for the three M_h regions. Again, the general trend is a slight rise in magnitude with respect to z. Interestingly, the $0.6 < M_h < 0.95$ GeV bin has significant, nonzero $|1,-1\rangle$ and $|2,-2\rangle$ amplitudes, especially at high z; the corresponding DiFFs to which these are sensitive involve correlations with the fragmenting quark transverse momentum, and so far have not yet been constrained.

4 Conclusion

Measurements of the beam spin asymmetry A_{LU} in SIDIS dihadron production are sensitive to dihadron fragmentation functions $G_1^\perp$ and H_1, dependent respectively on the longitudinal and transverse spin of the fragmenting quark. These functions expand in partial waves, each sensitive to the interference of dihadrons with particular polarizations. The presented measurement of partial wave amplitudes of A_{LU} refine access to $G_1^\perp$ extending the prior measurement [4] and allow for a better understanding of $H_1^{\sphericalangle}$ and $H_1^\perp$. Future measurements can include different dihadron channels, such as $K\pi$ and $\pi^0\pi^\pm$, which will probe different sets of fragmentation functions, as well as SIDIS from a deuteron target, which will help disentangle flavor dependence.

Acknowledgements

References

[1] A. Bacchetta and M. Radici, *Partial-wave analysis of two-hadron fragmentation functions*, Phys. Rev. D **67**, 094002 (2003), doi:10.1103/PhysRevD.67.094002.

[2] A. Bacchetta and M. Radici, *Two-hadron semi-inclusive production including subleading twist contributions*, Phys. Rev. D **69**, 074026 (2004), doi:10.1103/PhysRevD.69.074026.

[3] S. Gliske, A. Bacchetta and M. Radici, *Production of two hadrons in semi-inclusive deep inelastic scattering*, Phys. Rev. D **90**, 114027 (2014), doi:10.1103/PhysRevD.90.114027.

[4] None, *Observation of Beam Spin Asymmetries in the Process $ep \rightarrow e'\pi^+\pi^- X$ with CLAS12*, Phys. Rev. Lett. **126**, 152501 (2021), doi:10.1103/PhysRevLett.126.152501.

[5] C. A. Aidala, S. D. Bass, D. Hasch and G. K. Mallot, *The spin structure of the nucleon*, Rev. Mod. Phys. **85**, 655 (2013), doi:10.1103/RevModPhys.85.655.

[6] A. Metz and A. Vossen, *Parton fragmentation functions*, Prog. Part. Nucl. Phys. **91**, 136 (2016), doi:10.1016/j.ppnp.2016.08.003.

[7] M. Anselmino, A. Mukherjee and A. Vossen, *Transverse spin effects in hard semi-inclusive collisions*, Prog. Part. Nucl. Phys. **114**, 103806 (2020), doi:10.1016/j.ppnp.2020.103806.

[8] H. Avakian, B. Parsamyan and A. Prokudin, *Spin orbit correlations and the structure of the nucleon*, Riv. Nuovo Cim. **42**, 1 (2019), doi:10.1393/ncr/i2019-10155-3.

[9] A. Bacchetta, G. Bozzi, M. G. Echevarria, C. Pisano, A. Prokudin and M. Radici, *Azimuthal asymmetries in unpolarized SIDIS and Drell-Yan processes: A case study towards TMD factorization at subleading twist*, Phys. Lett. B **797**, 134850 (2019), doi:10.1016/j.physletb.2019.134850.

[10] A. Courtoy, *Insights into the higher-twist distribution $e(x)$ at CLAS*, arXiv:1405.7659.

[11] W. Yang, X. Wang, Y. Yang and Z. Lu, *Single-spin asymmetry in dihadron production in SIDIS off longitudinally polarized nucleon targets*, Phys. Rev. D **99**, 054003 (2019), doi:10.1103/PhysRevD.99.054003.

[12] S. A. Pereira, *Di-hadron production at Jefferson Laboratory*, Proc. Sci. **203**, 231 (2014), doi:10.22323/1.203.0231.

[13] S. Sirtl, *Azimuthal asymmetries in SIDIS di-hadron muoproduction off longitudinally polarized protons at COMPASS*, In 22nd International Symposium on Spin Physics (2017), arXiv:1702.07317.

[14] H. H. Matevosyan, A. Kotzinian and A. W. Thomas, *Accessing Quark Helicity through Dihadron Studies*, Phys. Rev. Lett. **120**, 252001 (2018), doi:10.1103/PhysRevLett.120.252001.

[15] A. Vossen et al., *Observation of transverse polarization asymmetries of charged pion pairs in e^+e^- annihilation near $\sqrt{s}$ = 10.58 GeV*, Phys. Rev. Lett. **107**, 072004 (2011), doi:10.1103/PhysRevLett.107.072004.

[16] A. Courtoy, A. Bacchetta, M. Radici and A. Bianconi, *First extraction of interference fragmentation functions from e^+e^- data*, Phys. Rev. D **85**, 114023 (2012), doi:10.1103/PhysRevD.85.114023.

[17] V. D. Burkert et al., *The CLAS12 Spectrometer at Jefferson Laboratory*, Nucl. Instrum. Meth. A **959**, 163419 (2020), doi:10.1016/j.nima.2020.163419.

[18] D. Van Ravenzwaaij, P. Cassey and S. D. Brown, *A simple introduction to Markov chain Monte–Carlo sampling*, Psychonom. Bull. Rev. **25**, 143 (2018).

[19] M. Bonamente, *Monte Carlo Markov Chains*, in Statistics and Analysis of Scientific Data, Springer New York, NY, ISBN 9781493965700 (2016), doi:10.1007/978-1-4939-6572-4_16.

[20] N. Metropolis, A. W. Rosenbluth, M. N. Rosenbluth, A. H. Teller and E. Teller, *Equation of State Calculations by Fast Computing Machines*, J. Chem. Phys. **21**, 1087 (1953), doi:10.1063/1.1699114.

[21] W. K. Hastings, *Monte Carlo sampling methods using Markov chains and their applications*, Biometrika **57**, 97 (1970), doi:10.1093/biomet/57.1.97.